Kodaikanal Obs. Bull. (1986) 6

OUR PRESENT UNDERSTANDING OF SOLAR FLARES

B.N. Dwivedi
APPLIED PHYSICS, I.T.
BANARAS HINDU UNIVERSITY
VARANASI 221 005

Abstract

A general discussion of solar flares with emphasis on two-ribbon flares is given. The basic differences between compact (simple-loop) and two-ribbon flares have also been pointed out. Skylab observations have been presented to show that the hot loops are seen first in X-rays, later in extreme ultraviolet lines and, after an appropriate cooling time, in Hα as the loop prominence systems. Particle acceleration during a long-enduring reconnection process in two-ribbon flares have been discussed.

General Discussion of Solar Flares

The solar flare represents a sudden release of energy in the surrounding regions of the sun. It is a fascinating, complex and highly informative phenomena. The solar flares emit electromagnetic radiations and eject charged particles. Different regions of the electromagnetic spectrum contain different information of flaring region. Therefore, one must assemble a composite picture of the flare by observing its manifestations right across the electromagnetic spectrum. Some of the morphological features of solar flares are evidently shown in Fig.1.

For several decades flares were observed in Hα light as a sudden brightenings of the chromospheric active regions. The Hα flare differed in their size and brightness but they were believed to be occurring through the same process of instability on different scales on the sun. Radio observations for the first time showed that specific types of radio burts were associated with some particular flares whereas other Hα flares did not show them. This distinction became more obvious from space-borne observations. It was found that intense streams of atomic nuclei and relativistic electrons in space were coming from flares associated with type II and IV radio bursts. On the other hand non-relativistic electrons were found to be closely linked with type III radio burst.

Spacecraft observations showed another difference among Hα flares. Whereas some flares emit only soft X-rays in the form of a gradual, long-lasting burst; the other flaring events produce a hard X-ray burst of short duration followed by or superimposed on the soft X-ray emission. In some flares the hard X-ray burst dominates the event. Finally there are flares which repeatedly emit hard X-rays for minutes or even tens of minutes. All these observations suggest that there may be different processes involved in different flares. However, a flare is primarily a coronal phenomenon. The secondary effects of flares are seen in the Hα lights in the chromosphere. Thus the pictures of different flaring events in the corona were needed. These observations were obtained from Skylab in 1973.

Skylab Observations

Skylab yielded flare images in soft X-rays from above 3 Å to about 50 Å i.e. in the energy range up to 4 keV. It also gave flare images in ultraviolet lines exhibiting

the flare in the transition layer and corona. Thus for the first time it was possible to get the real three dimensional images of flares instead of their footprints in the chromosphere.

The Skylab Flare Workshop (Moore et al., 1980; Svestka, 1981) has shown that there are at least two different kinds of flare events. The first kind belongs to compact flares (simple-loop flares or static flares) in which a pre-existing loop or a system of loops (emerging or exceedingly twisted) is excited without any apparent microscopic dynamics of the flaring loops. The flare life time is compatible with a short-lived impulsive energy input and subsequent cooling. The second kind of flares concern the two-ribbon flares (dynamic flares) in which new loops appear subsequently in emission and the loop system grows during the flare development. The life time greatly exceeds the radiative cooling time so that a long-lasting continuous energy input is needed. Thus we can expect that the hard X-rays, which mainly reveal the impulsive energy input, may be different in these two classes of flares. The Skylab observations of course, did not include coverage of the hard X-ray spectral region ($h\nu \geq 20$ keV). Some examples of compact and two-ribbon flares in hard X-rays are shown in Figs. 2 & 3.

Two-Ribbon Flares

Using simultaneous ISEE 3 hard X-ray record and high-resolution Big Bear Hα movies and the information contained in the NOAA Solar Geophysical Data Bulletin, Dwivedi et al. (1984) suggested the following:

1. A two-ribbon flare is preceded in Hα by the activation and disruption of an active-region filament. This criterion may be negative for some two-ribbon flares when no filament is discernible at the flare site before the flare onset (in young regions or its previous disruption) but this is negative for all compact flares.

2. Two (or more) bright ribbons are seen in Hα, and these two-ribbons drift apart, with $H_{\parallel}=0$ line between them. This motion can be stopped by the strong longitudinal fields in sunspots, but at least part of the ribbons should be seen moving. This motion is usually quite fast in the onset phase of the flare, whereas the compact flare patches (which may occasionally resemble 'two-ribbons') do not move.

3. A two-ribbon flare is accompanied by metric ratio bursts of type II and/or IV. There are definitely two-ribbon flares where these radio emissions (or one of them) are missing (cf. Svestka 1976, for a discussion of the reasons for that); thus this criterion may be negative for some two-ribbon flares. However, this criterion is negative for all compact flares.

4. Hard X-ray bursts associated with two-ribbon flares are invariably long-lasting of duration > 1 min) and complex.

The exact process of triggering the filament activation in a two-ribbon flare is not yet known. It is likely that a newly emerging magnetic flux nearby which changes the magnetic configuration, or the growth of a coronal hole, which opens the magnetic field; or a travelling disturbance from another part of the sun, which hits the magnetic field configuration and deforms it. After the filament disappears in the Hα, we see in X-rays a system of growing loops, with maximum brightness at their tops where temperature exceeds 10^7 K. In Hα, we see two bright ribbons aligned with the $H_{\parallel}=0$ line extending the footprints of the hot coronal loops. Sometime later, the system of cool loops, with temperature of the order of 10^4 K, rooted at the inner edges of the bright ribbons are seen.

The Flare of 1973 July 29

This major two-ribbon flare in a spotless active region is the best example of a big two-ribbon flare observed on Skylab (Fig.4). Unfortunately the soft X-ray observations started 3 hours after the onset of the flare. However, they still showed very well the growing system of coronal post-flare loops, with temperature at the top in excess of 5×10^6 K. In a series of papers on the flare of 1973 July 29 (Nolte et al. 1979; Martin, 1979; Svestka et al. 1982a), it has been shown that Hα "post-flare" loops are the cooled aftermath of previously hot coronal loops which were visible in X-rays in the same position earlier in the flare. Kopp and Pneuman (1976) have proposed that these post-flare loops are formed by a process of successive magnetic field reconnections of previously distended magnetic field lines as illustrated in Fig.6. The filament disruption marks an opening of the originally closed magnetic field. Solar wind begins to flow along the open lines so that gas pressure inside the opened filament cavity decreases. Thus magnetic pressure prevails and drives the open field lines towards the neutral sheet in the central of the disrupted cavity, where field lines begin to reconnect. The reconnection starts at the bottom of the disrupted configuration and the neutral point then propagates upwards, creating progressively higher loops. The process of reconnection is very fast in its initial phase, but it progressively slows down as the neutral point rises with decreasing speed through corona.

When a bunch of field lines reconnects and a new coronal loop is formed, the upward streaming along the field lines is suddenly stopped. Consequently, a shock is produced at the top of the loop which travels downwards and can heat the loop to some 3 or 4×10^6 K. In addition, the loop is heated at the top - where the reconnection were accomplished - by the reconnection process itself, probably through Ohmic dissipation of the magnetic field energy at the reconnection site (Pneuman 1981). The heat is conducted downwards, heats the chromosphere and produces the two bright chromospheric ribbons. Some part of the heat chromospheric gas evaporates into the loop, thus enhancing its density. Accelerated particles may also be involved in this process of chromospheric heating (Svestka et al. 1980). One needs to add mass to the loop system, because otherwise there is no enough plasma in the corona to make the cool Hα loops visible (Kleczek 1963; Jefferies & Orrall 1963).

Soon after the reconnection is accompalished the newly formed coronal loops in soft X-rays is seen (Moore et al. 1980). The loop then cools and after sometime ceases to be visible in X-rays and becomes visible in various EUV lines with decreasing temperature. At the end the loop can be seen in Hα. It has been very nicely demonstrated for the limb event of 1973 August 14 (MacCombie & Rust, 1979) where simultaneous observations (Fig.6) were available in different lines: He II ($T < 10^5$ K), Ne VII ($T \simeq 5 \times 10^5$ K), Mg IX ($T \simeq 9 \times 10^5$ K), Fe XV ($T \simeq 2 \times 10^6$ K), Fe XVI ($T \simeq 3 \times 10^6$ K) and soft X-rays ($T > 1.5 \times 10^6$ K).

The Kopp and Pneuman model has several key features in commdn with some other reconnection models which make it an attractive model for two-ribbon flares in general (Svestka et al. 1980). As illustrated in Fig.7, Skylab observations have shown that loops are the fundamental form of the coronal part of EUV and X-ray flares. Secondly, when reconnection occurs, high energy particles and/or thermal waves would be accelerated along the lower half of the reconnected magnetic field. The impact of such particles and/or heat waves with the chromosphere can produce the typical two-ribbon flares.

Particle Acceleration

Two-ribbon flares have been shown to be powerful source of particle acceleration (Svestka 1976). The first three well observed gamma-ray flares (1972 August 4 and 7; 1978 July 11) were two-ribbon flares and duration of their hard X-ray emission was quite extended (cf. Chupp et al. 1973; Hoyng et al. 1976; Hudson et al. 1980).

The appearance of impulsive hard X-ray and microwave bursts during the initial, flash phase of the flare reveals that the acceleration process starts very close to the onset of the flare development. Almost simultaneously with hard X-rays, with a delay shorter than one minute, major flares also emit the gamma ray line at 2.2 MeV (Hudson et al. 1980). However, this (neutron) line needs atomic nuclei with energy in excess of 30 MeV for its production (Ramaty et al. 1977) and its formation must be delayed because of the atomic processes involved by at least 30 sec (Wang & Ramaty 1974). Thus the acceleration process in the earliest phase of the flare development should be able to accelerate protons to energies in excess of 30 MeV.

A question arises, by which process this initial acceleration is accomplished. There are essentially two alternatives: either the acceleration occurs when the filament disrupts, in which case current interruption and shock-associated acceleration seem to be the most likely processes, or the acceleration starts when the first loops are formed, in which case it should be associated with the process of reconnection.

The fact that the impulsive bursts are seen only after the onset of the visible flare i.e. after the reconnection has started, strongly favours the second alternative. Besides, simultaneously with the gamma-rays we also see flare white light emission (Fig.8) which is caused by accelerated particles, penetrating to the low chromospheric layers (Svestka 1970; Najita & Orrall 1970; Hudson & Dwivedi 1982). The white-light flare patches are clearly the foot-points of one or more coronal loops. Thus a significant fraction of the accelerated particles must be confined to the flare loops and this can most easily happen if the particles are accelerated at the reconnection site (Svestka et al. 1980). Then a fraction of the particles is trapped in the reconnected loop while another part propagates upwards and can be accelerated to still higher energies in the flare produced shock wave. Figure 9 shows a model of a two-ribbon flare event as it has been schematically proposed by Svestka et al. (1980). Thus one can suppose that at any time when a new loop reconnects, particles are accelerated to enhanced energies. The most energetic particles are produced when the first loops are formed very low in the corona; after that the peak energy of the accelerated particles decreases as the reconnection process slows down. But one can see that the whole acceleration process proceeds for hours. In long-lasting post-flare loopevents, like that of 1973 July 29, some particles would still be accelerated 12 hour after the flare onset (Svestka et al. 1980).

Dwivedi et al. (1984) studied the acceleration process in the corona, as it is manifested by the impulsive hard X-ray bursts at the flare onset. Their conclusions can be summarized as follows:

1. Essentially all two-ribbon flares that produce hard X-rays are characterized by complex, long lasting hard X-ray bursts (Fig.4). In contrast the compact flares tend to be associated with isolated, single peaks in hard X-rays (Fig.3). This seems to confirm that there is a long-lasting acceleration process in the two-ribbon flares, whereas the acceleration in compact flares is impulsive and short-lived.

2. However, even major two-ribbon flares need not necessarily produce hard (>20 keV) X-rays, if the filament eruption and the two-ribbon formation occurs far from the strong magnetic fluxes in sunspots.

3. The individual peaks in the hard X-ray bursts seem to be closely related to sunspot proximity. At least in some events these peaks appear at the times when new Hα emission is seen in penumbrae of sunspots. This was the case, e.g., at the peaks shown in Figs.4a, b, c. Separate spikes may correspond to brightenings at different sunspots, sometimes quite far apart.

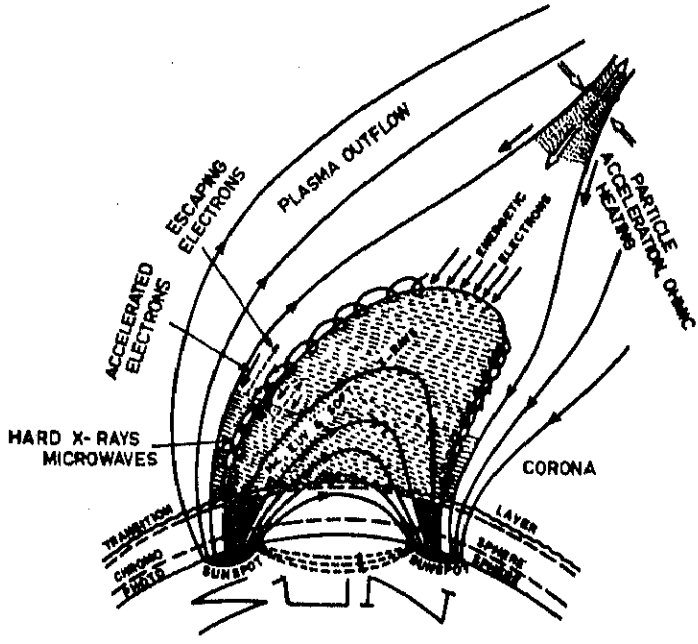

Fig.1. Schematic flare model.

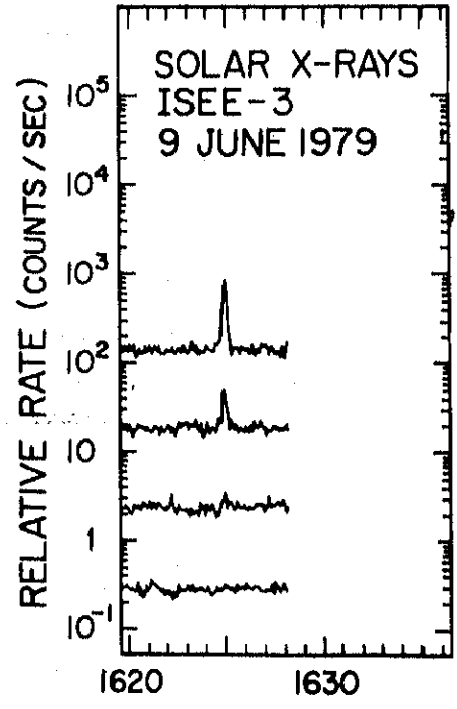

Fig.2. ISEE-3 hard X-ray records of the emission from compact flare, June 9, 1979 (Hα importance SB).

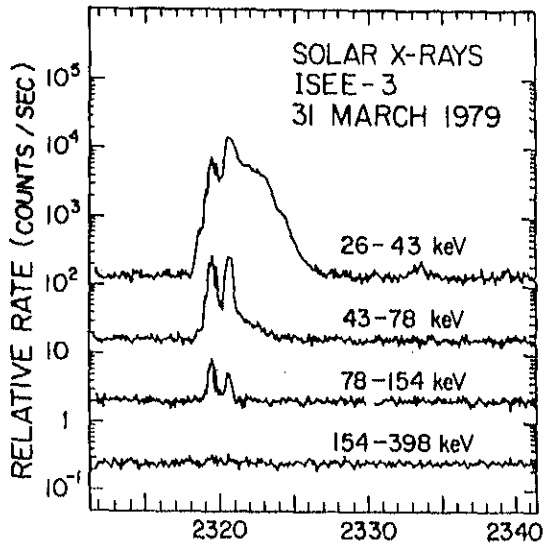

Fig.3. ISEE-3 hard X-ray records of the emission from two-ribbon flare, 1979 March 31.

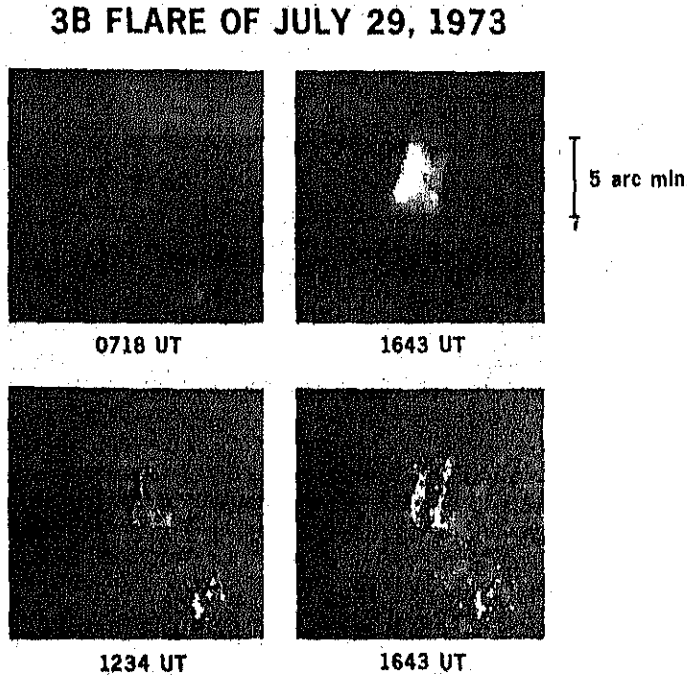

Fig.4. Soft X-ray pictures (3-54 Å, above) and Hα photographs (below) of the preflare situation (left) and the flare emission at 16:43 UT on 1973 July 29 (right). The hot X-ray loops, with maximum brightness and temperature at the top, are rooted in the chromospheric bright ribbons that extend along both sides of the disappeared dark filament.

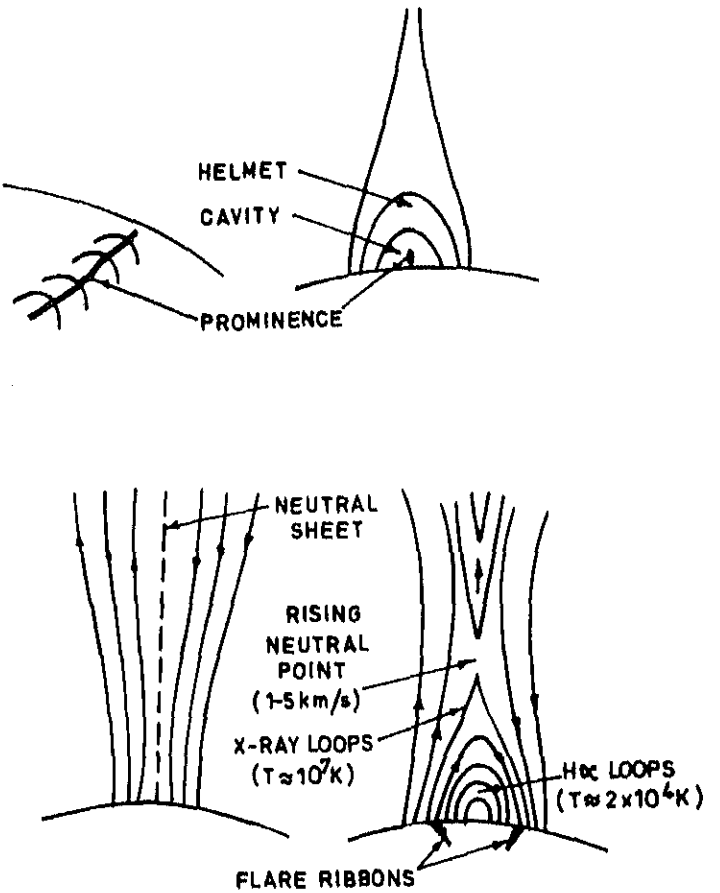

Fig.5. Kopp and Pneuman (1976) for post-flare loops. In the quiet situation (top) the filament is embedded in a coronal cavity below a helmet of higher lying loops. An instability opens the magnetic field and the filament disappears (lower left). The field topology at some arbitrary time during the flare (lower right). Here the open field is reconnecting to form closed loops with the hottest at the top where the magnetic energy is being released, and the cool (Hα) loops lower down. These cool loops were formerly hot but have lost most of their thermal energy content due to radiation and thermal condution. The chromospheric flare ribbons are presumably produced by energy travelling downward (via either thermal conduction or energetic particles) from the reconnecting region.

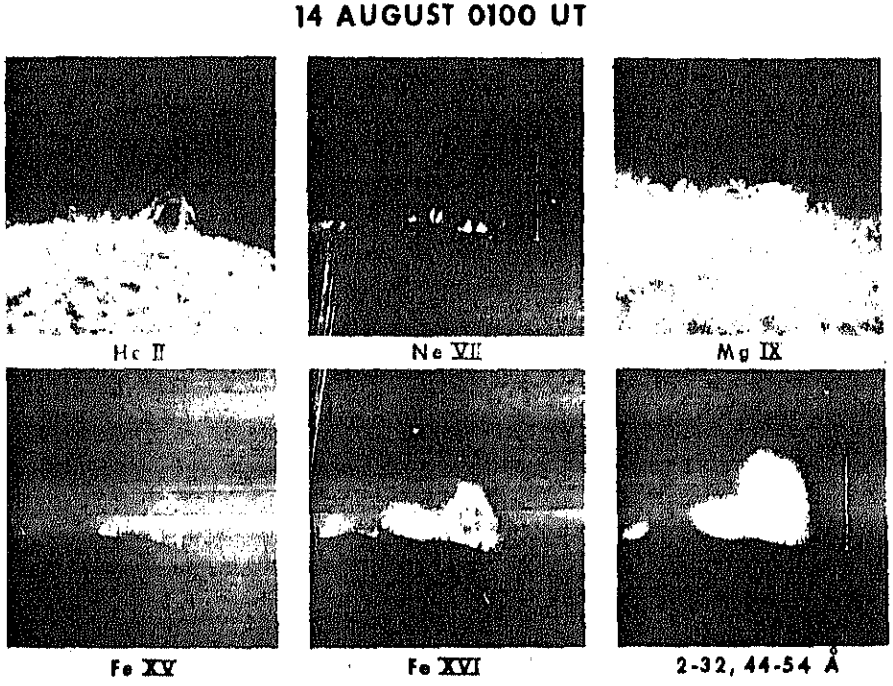

Fig.6. Simultaneous EUV pictures and an X-ray picture of a system of loops seen on the limb after a filament disruption (1973 Aug. 14; 0100 UT). All pictures are on the same scale. The vertical line on the Ne VII and X-ray pictures shows the much higher extension of the X-ray loops (After MacComble & Rust, 1979).

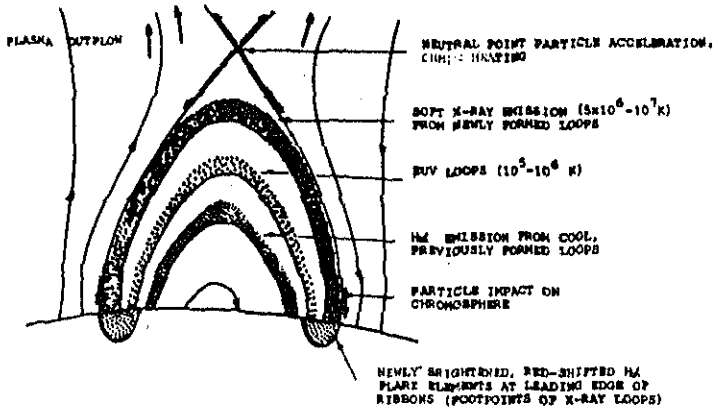

Fig.7. Interrelationship of various coronal flare loops and the chromospheric flare (After Svestka et al. 1980).

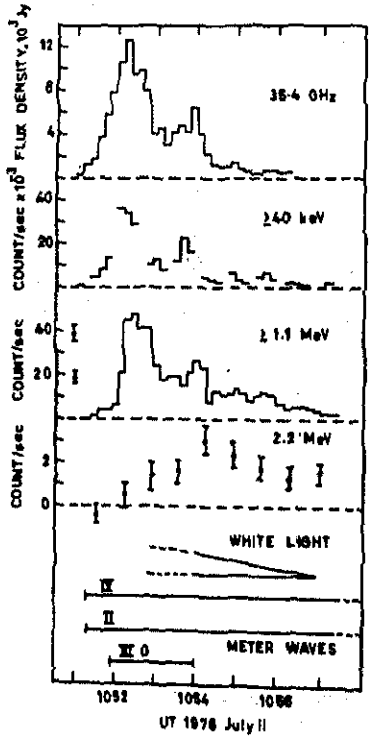

Fig.8. A comparison of time profiles of the microwave impulsive burst (35.4 GHz), hard X-rays (>40 keV), gamma-ray continuum (>1.1 MeV), the neutron gamma-ray line at 2.2 MeV, and the white-light emission (Debrecen) in the gamma-ray flare of 1978 July 11 (After Hudson et al. 1980).

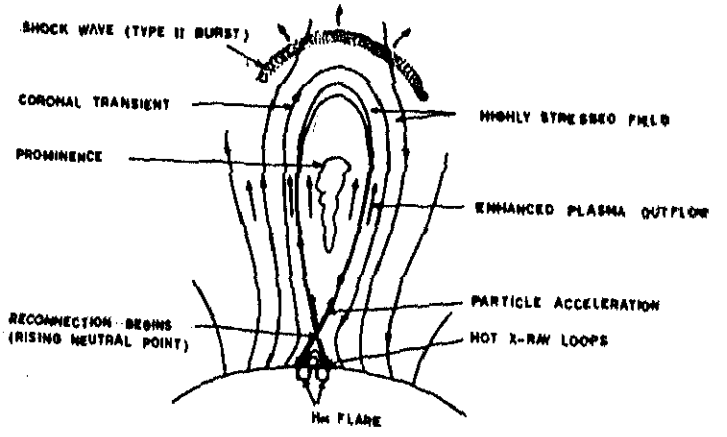

Fig.9. Schematic drawing of the initial phase of a two-ribbon flare (After Svestka et al. 1980).

1980 May 21 Flare

The major two-ribbon flare of 1980 May 21 is one of the best observed and studied flare on record. The observations of this flare from SMM spacecraft provided the first study of images of hard X-ray brightenings at footprints of loops during impulsive phase (Hoyng et al. 1981). The giant post-flare coronal arches following two-ribbon flares were discovered (Svestka et al. 1982b). The high-velocity upward motions was found during the impulsive phase giving information about the early phase of chromospheric evaporation (Antonucci et al. 1985). A direct evidence for a late energy release high in the corona was found during the growth of post-flare loops. This was interpreted to be the hard X-ray images of the reconnection of field lines.

Closing Remarks

This review presents in an introductory way some of the aspects of solar flares as understood from earlier space-borne observations. Solar Max observation of 1980 May 21 flare has been presented in ordear to highlight the latest efforts continuing to solve the flare puzzle. As we see, only one kind of flare tells a lot about it adding new dimensions to our present understanding of the flare phenomenon. This also shows how complex the phenomenon is if one ever gets on to learn about it in toto.

Acknoweldgement

The author is grateful to Professor Zdeněk Švestka for kindly sending his work on May 21 flare.

References

Antonucci, E., Dennis, B.R., Gabriel, A.H. and Simnett, G.M. 1985. Solar Phys. **96**, 129.
Chupp, E.L., Forrest D.J., Higbie, P.R., Suri, A.N., Tsai, C. and Dunphy, P.P. 1973. Nature, **241**, 333.
Dwivedi, B.N., Hudson, H.S., Kane, S.R. and Svestka, Z. 1984. Solar Phys. **90**, 331.
Hoyng, P., Brown, J.C. and van Beek, H.F. 1976. Solar Phys. **48**, 197.
Hoyng, P., Duijveman, A., Machado, M.E., Rust, D.M., Svestka, Z., Boelee, A., de Jager, C., Frost, K.J., Lafleur, H., Simnet, G.M., van Beek, H.F. and Woodgate, B.E. 1981. Astrophys. J. **246**, L155.
Hoyng, P. 1982. The Observatory, **102**, 119.
Hudson, H.S., Bai, T., Gruber, D.E., Matteson, J.L., Nolan, P.L. and Peterson, L.E. 1980. Astrophys. J. **236**, L91.
Hudson, H.S. and Dwivedi, B.N. 1982. Solar Phys. **76**, 45.
Jefferies, J.T. and Orrall, F.Q. 1963. In the Solar Spectrum (ed. C. de Jager), p.245.
Kleczek, J. 1963. Bull. Astr. Inst. Csl. **14**, 147.
Kopp, R.A. and Pneuman, G.W. 1976. Solar Phys. **50**, 85.
MacCombie, W.J. and Rust, D.M. 1979. Solar Phys. **61**, 69.
Martin, S.F. 1979. Solar Phys. **64**, 165.
Moore, R., McKenzie, D.L., Svestka, Z., Widing, K.G. and 12 co-authors. 1980, in P.A. Sturrock (ed.), Solar Flares, Proceedings of the Second Skylab Workshop, Colorado Assoc. Univ. Press, p.341.
Najita, K. and Orrall, F.Q. 1970. Solar Phys. **15**, 176.
Nolte, J.T., Gerassimenko, M., Krieger, A.S., Petrasso, R.D. and Svestka, Z. 1979. Solar Phys. **62**, 123.
Pneuman, G.W. 1981. In E. Priest (ed.), Solar Flare Magnetohydrodynamics, Gordon and Breach, New York.
Ramaty, R., Kozlovsky, B. and Suri, A.N. 1977. Astrophys. J. **214**, 617.
Svestka, Z. 1970. Solar Phys. **13**, 471.
Svestka, Z. 1976. Solar Flares, Dordrecht: D. Reidel.

Svestka, Z., Martin, S.F. and Kopp, R.A. 1980. IAU Symp No.91, 217.
Svestka, Z. 1981, in E. Priest (ed.), Solar Flare Magnetohydrodynamics, Gordan and Breach, New York, p.47.
Svestka, Z., Dodson-Prince, H.W., Martin, S.F., Mohlet, O.C., Moore, R.L., Nolte, J.T. and Petrasso, R.D. 1982a. Solar Phys. 78, 271.
Svestka, Z., Stewart, R.T., Hoyng, P., van Tend, W., Acton, L.W., Gabriel, A.H., Rapley, C.G. and 8 co-authors. 1982b. Solar Phys. 75, 305.
Wang, H.T. and Ramaty, R. 1974. Solar Phys. 36, 129.